# ORGANIC HETEROSTRUCTURES DEPOSITED BY MAPLE ON PATTERNED AZO ELECTRODES

M. SOCOL[a,*], N. PREDA[a], C. BREAZU[a], O. RASOGA[a], A. STANCULESCU[a], G. POPESCU-PELIN[b], F. GHERENDI[b], G. SOCOL[b], L. VACAREANU[c]
[a]*National Institute of Material Physics, 405AAtomistilor Street, 077125, Bucharest-Magurele, Romania*
[b]*National Institute for Lasers, Plasma and Radiation Physics, 409 Atomistilor Street, 077125, Bucharest-Magurele, Romania*
[c]*P.Poni Institute of Macromolecular Chemistry, 41 A Gr. GhicaVoda Alley, 700487-Iasi, Romania*

The paper is focused on the investigation of the properties of some organic heterostructures deposited on patterned AZO electrodes. In the first step, 2D patterned arrays based on commercially photoresist were fabricated on glass substrates using nanoimprint litography. Next, on these periodic nanostructures, the transparent AZO layers were deposited by pulsed laser deposition. Further, heterostructures consisting in organic thin films such as 4,7 diphenyl-1,10-phenanthroline (BPhen) (electron transport layer), N,N'-di(1-naftalenil)-N,N'-diafenil-(1,1'-bifenil)-4,4'-diamina (α-NPD) (hole transport layer) and arylenevinylene oligomers (3,3-bis (N-hexylcarbazole)vinylbenzene (P13) and 1,4-bis [4-(N,N-diphenylamino)phenylvinyl] benzene (P78)) were obtained by matrix assisted pulsed laser evaporation. The fabricated multilayer organic structures have been investigated from optical (UV-VIS spectroscopy), morphological (scanning electron microscopy and atomic force microscopy) and electrical (I-V characteristics) point of view. An improvement in the current value recorded on the samples prepared on nanostructured electrode was recorded. The results evidence the possibility to integrate these heterostructures in organic electronic devices.

(Received August 8, 2018; Accepted October 31, 2018)

*Keywords: nanostructures, UV-NIL, AZO, organic heterostructures, MAPLE*

## 1. Introduction

Over the last few decades, organic and inorganic semiconductors were used in devices for electronic and optoelectronic applications such as solar cells, thin film transistors, light emitting diodes, photodetectors, field effect transistors, and so on [1-10]. Due to the features like transparency, high flexibility (compatibility with plastic substrates) or high absorption coefficients, a particular interest was paid to the organic compounds, their main applications remaining organic light emitting devices (OLED), organic solar cells (OSC), field effect transistors based on organic material (OFET), photodetectors, etc. [11-15]. OLEDs especially attracted attention due to some advantages such as: high luminous power efficiency, fast response time, colours purity or flexibility, these being already integrated in flat or flexible monitors and in lighting devices [11, 12, 16].

Various factors must be taken in consideration when the organics are chosen for the fabrication of OLED structures. Thus, adequate charge carrier transport properties, photoluminescence, appropriate value of the ionisation potential (IP) and electron affinity (EA) play an important role in the preparation of a heterostructure with low energetic barrier at the transparent conductive electrode (TCE)/ organic, organic/organic and organic/metal interfaces [17]. N,N′-Bis(3-methylphenyl)-N,N′-diphenylbenzidine (TPD) or N,N′−diphenyl−N,N′−bis(1−naphthyl)−1,1′−biphenyl−4,4′−diamine (α-NPD) are the most used hole-transport layers

*Corresponding author: marcela.socol@infim.ro

(HTL). As emissive layer, 5,12-Dihydro-5-12-dimethylquino[2,3-b]acridine-7,14dione (DMQA), tris-8-hydroxyquinoline aluminium ($Alq_3$) are usually involved. 2-(4-tert-Butylphenyl)-5-(4-biphenylyl)-1,3,4-oxadiazole (PBD) or 2,9-Dimethyl-4,7-diphenyl-1,10-phenanthroline (BCP) can be used as electron-transport layers (ETL) [16,18].

In the field of the organic materials there is a great interest to develop new compounds with adequate propertiesby molecular design [18].

Vacuum thermal evaporation (VTE) is the most used method to obtain organic thin films for OLED applications [16]. Matrix assisted pulsed laser evaporation (MAPLE) is another technique employed in the deposition of these soft organic materials. Until now this method was principally used in the field of organic solar cell (OSC) applications. This laser technique works with a frozen target, lower laser fluences (under 500 $mJ/cm^2$) and can assures the transfer of the organic compounds without deterioration of the chemical structure of the raw materials [19-21].

In the OLEDs structures, indium tin oxide (ITO) remains the most used transparent electrode. However, due to the increased price of the indium there is the tendency to find others oxides which could replace ITO in these types of applications but with similar optical and electrical properties [14, 22]. The most investigated TCE were those based on ZnO:In:ZnO (IZO), Al:ZnO (AZO), Ga:ZnO (GZO) [14, 23-26]. From these materials, AZO was used with success in OLEDs domain, some papers reporting devices prepared on AZO as TCE with comparable performances with those obtained on ITO [12, 16]. Additionally, using a patterned electrode there is the possibility to increase the mobility of the charge carrier in the prepared organic heterostructures [27].

The aim of this study is to evidence the influence of TCE patterned electrode on the electrical properties of the organic heterostructures fabricated on it. Thus, new organic compounds (arylenevinylene oligomers) were deposited by MAPLE on AZO patterned electrode. The morphological, optical and electrical properties of this organic heterostructure were compared with those obtained for the same heterostructure deposited on AZO flat electrode.

## 2. Experimental

Pillar nanostructures (NS) were obtained on glass substrate by UV nanoimprimt litography (UV-NIL) technique involving the following steps: preheating of the glass substrate for 2 min at 150 $^oC$, deposition of the primer (for a better adhesion of the resist) on the glass by spin-coating (Brewer Science Cee 200X Spin Coater), spin-coating of the UV-resist on the primer, thermal treatment of the obtained layer at 120 $^oC$ for 30 s, pressing of a soft stamp with the desired model (EVG 620 mask aligner) on the resist with a uniform contact pressure (100 mbar), exposure of the resist at the UV light for 90 s for its solidification, removing of the stamp. More details regarding the UV-NIL obtaining process can be found in the reference [28].

The AZO films were deposited on both NS/glass and flat glass by pulsed laser deposition (PLD) method using an excimer laser source with KrF* (Coherent, Compex Pro 205, operating at λ=248 nm). ZnO doped with 2% Al solid target (SCI Engineering Materials) was implied in the deposition of the transparent layers, the following conditions being used: 8 cm substrate-target distance, $2J/cm^2$ laser fluence, 8000 number of the pulses, 1 Pa pressure of the oxygen atmosphere [29]. The electrical resistivity of the prepared samples was measured with a Jandel four point probe head and was determined as being 2.4xE-4 Ωcm.

*Table 1. MAPLE deposited organic heterostructures indexation, target concentration, number of the laser pulses and roughness parameters (root mean square-RMS and roughness average-$R_a$) evaluated from the AFM measurements.*

| Indexation | Structure | Target (%) | No. of pulses | RMS (nm) | Ra (nm) |
|---|---|---|---|---|---|
| P1 | AZO/NPD/LS13/BPhen | 3/1/3 | 25k/15k/15k | 53 | 38 |
| P2 | AZOnan/NPD/LS13/BPhen | 3/1/3 | 25k/15k/15k | 77 | 62 |
| P3 | AZO/NPD/LS78/BPhen | 3/1/3 | 25k/15k/15k | 90 | 67 |
| P4 | AZOnan/NPD/LS78/BPhen | 3/1/3 | 25k/15k/15k | 95 | 76 |

MAPLE was used to deposit three different organic films on AZO, in this configuration: N,N'-di(1-naftalenil)-N,N'-diafenil-(1,1'-bifenil)-4,4'-diamina (α-NPD), 3,3-bis (N-hexylcarbazole)vinylbenzene (LS 13) or 1,4-bis [4-(N,N-diphenylamino)phenylvinyl] benzene (LS 78) and 4,7 diphenyl-1,10-phenanthroline (BPhen). By MAPLE, successive organic films from the same solvent can be obtained without the degradation of the preliminary deposited layer. The implied laser source was the same with that used in the PLD deposition. For each deposition, a frozen target containing the organic material and dimethyl sulfoxide (DMSO) was prepared. Four different samples (Table 1) were obtained, the following conditions being used: 5 cm substrate-target distance, 250mJ/cm$^2$ laser fluence [19]. In Fig. 1 is presented a schematic representation of the fabricated organic heterostructures (with LS 13 or LS 78 as intermediate layer) on flat and on patterned electrode. The thickness of the organic heterostructures obtained on flat electrode was evaluated (AmbiosProfilometer) at 300 nm for that containing LS13 and at 400 nm for that with LS78.

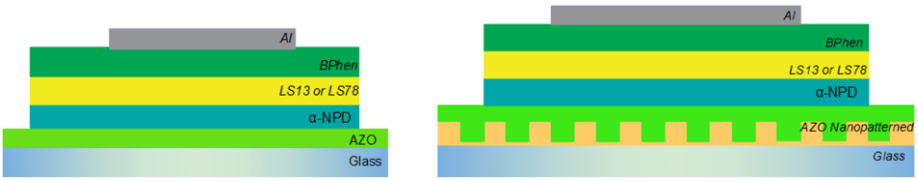


*Fig. 1. Schematic representation of the prepared organic heterostructures: on flat substrate (left) and on patterned substrate (right).*

In order to investigate the electrical properties of the organic heterostructures, an aluminium (Al) electrode (~ 100 nm) was deposited by vacuum evaporation (Spectros system from Kurt J. Lesker) on the top of the last organic layer.

Scanning electron microscopy-SEM (Zeiss Merlin Compact field emission scanning electron microscope) and atomic force microscopy-AFM (Nanonics Multiview 4000) were used to analyze the samples from morphological point of view.

The UV-VIS spectra were collected with a Carry 5000 Spectrophotometer, between (300 – 1000) nm for the TCE and (350-1000) nm for the organic layers. FTIR investigations were made with a Shimadsu 800 Spectrometer in order to obtain information about the preservation of the chemical structure of the raw materials (α-NPD, LS13, LS78 and BPhen) during the deposition process.

Current-voltage (I-V) characteristics were recorded in dark with a Keithley 2611A Source Meter Unit coupled at 2 microprobe Zuss PH-100.

## 3. Results and discussion

The morphology of the imprinted structures was investigated by SEM and AFM techniques. Thus, SEM images (Fig. 2 and Fig. 3) reveal pillar periodic nanostructures when NIL process is applied on glass substrates. The distance between two pillars is ~1150 nm, the pillar diameter is ~350 nm and the height is ~250 nm (value estimated from AFM images collected on the nanopatterned glass – Fig. 3). As was expected, when the AZO transparent electrode covers the pillars, no major changes seem to appear in the SEM image (Fig. 3). Only an increase in the pillars diameter has been evidenced. Comparing the AZO layer deposited on NS with that deposited directly on glass, a smooth surface is evidenced in the last case (Fig. 3).

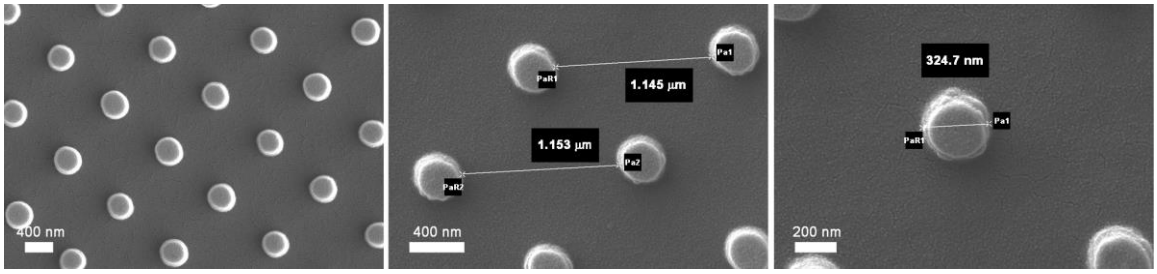


*Fig. 2. SEM images of the UV-NIL obtained pillars (left), estimated distance between pillars (middle), estimated diameter of the pillars (right).*

Further, the AFM scans (Fig. 3) sustain the SEM results, the periodic NS being evidenced in the topographic images recorded on NS and on AZO/NS. At the deposition of the AZO layer on the NS, a lowering in the Z value (188 nm) was remarked in comparison with the sample without AZO (248 nm). Probably, the gap between pillars is partially filled, resulting in a decrease of the Z value. In the case of the AZO layer deposited directly on glass, the Z value has just 70 nm, this being in agreement with previously results reported for this electrodedeposited by PLD [29].

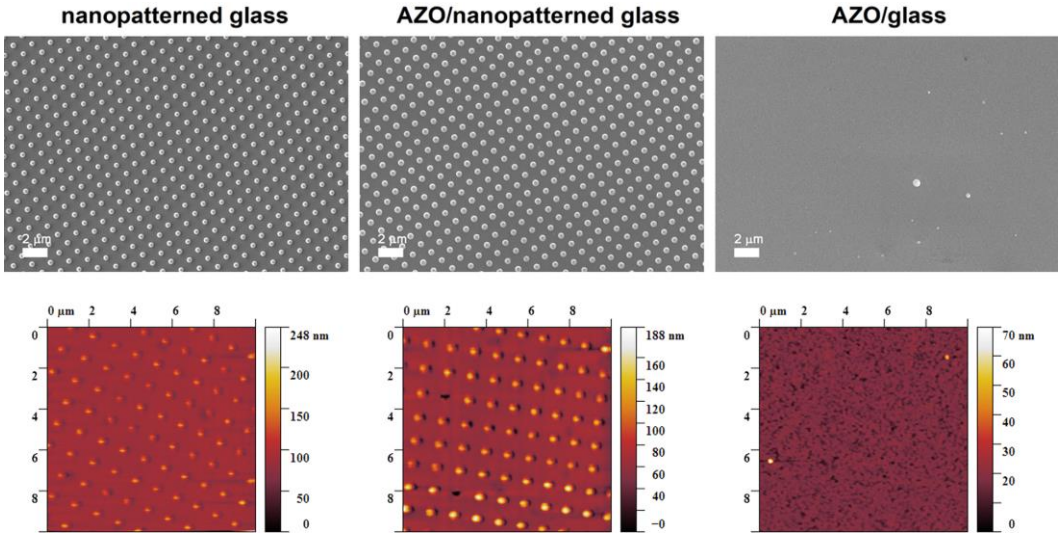


*Fig. 3. SEM and AFM images of: nanopatterned glass, AZO/nanopatterned glass and AZO/glass.*

In order to evidence the possibility to use AZO/NS/glass and AZO/glass as transparent electrodes for the preparation of the organic heterostructures, the UV-VIS spectra were recorded (Fig. 4). The transmittance of the NS/glass is lower in comparison with that of the glass substrate, having a special behaviour in the (350-750) nm domain related with the presence of some scattering phenomena [28]. The oscillations presented in the spectrum of the AZO layer deposited on glass appeared as the result of the light interference at air/TCE and TCE/glass interfaces, being characteristic for this material deposited by PLD or other techniques [29, 30]. For the AZO/NS sample, the shape of the UV-VIS spectrum is the same with that recorded for the NS/glass.

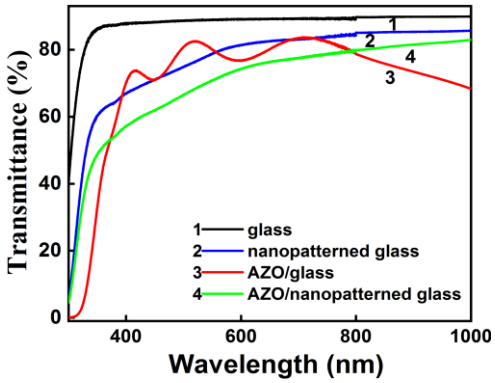


*Fig. 4. UV-VIS spectra of the AZO (deposited on NS or on glass) and of used reference samples (glass and NS/glass).*

The FTIR spectra were done on the films deposited on Si and are given in the Fig. 5. α-NPD is a material containing 78 atoms which presents a large number of vibrations. A major part of these were identified at about: 522 $cm^{-1}$ (C-C torsion or deformation), 567 $cm^{-1}$ (C-C torsion in biphenyl and naphtyl), 695 $cm^{-1}$ (C-C torsion in t-phenyl), 750 $cm^{-1}$(C-H wagging in t-phenyl), 775 $cm^{-1}$, 801 $cm^{-1}$and 957 $cm^{-1}$ (C-H wagging in naphtyl), 822 $cm^{-1}$(C-H wagging in phenyl), 1017 $cm^{-1}$(ring deformation), 1044 $cm^{-1}$(C-H bend and C-C deformation), 1085 $cm^{-1}$(C-H bend and C-C stretch in t-phenyl and naphtyl), 1181 $cm^{-1}$ (C-H bend and C-C stretch in biphenyl), 1250 $cm^{-1}$ (C-c stretch, C-H bend and C-N stretch in naphtyl), 1292 $cm^{-1}$(C-H bend, C-H strech), 1312 $cm^{-1}$(C-H bend, C-N stretch, C-C-N bend in phenyl),1399 $cm^{-1}$(C-C stretch, C-H bend in naphtyl), 1464 $cm^{-1}$ (C-C and C-N stretch, C-H bend innaphtyl), 1494 $cm^{-1}$ (C-C and C-N stretch, C-H bend in phenyl), 1574 $cm^{-1}$ (C-C stretch in naphtyl) [31].

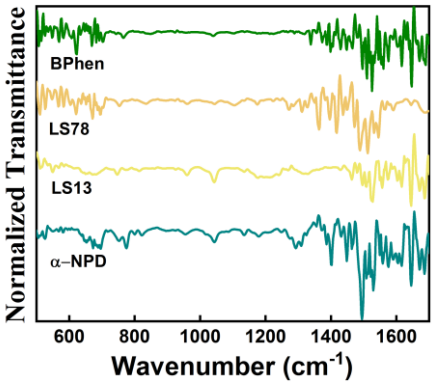


*Fig. 5. FTIR spectra of the organic thin films deposited by MAPLE.*

The arylenevinylene oligomers are also featured by characteristic vibrations. Thus, for the LS13 the following IR peaks at around: 813 $cm^{-1}$ (γ CH p-substituted benzene ring), 961 $cm^{-1}$ (HC=CH trans out-of-flat bending), 1146 $cm^{-1}$ (–C–N stretching), 1345 $cm^{-1}$ (=C–N chromophor), 1479 $cm^{-1}$,1495 $cm^{-1}$ and 1600 $cm^{-1}$ (ν C–C monosubstituted benzene) were identified. The LS78 reveals IR peaks at about: 695 $cm^{-1}$ (δ C–H phenyl rings), 833 $cm^{-1}$ (γ CH p-substituted benzene ring), 961 $cm^{-1}$ (HC=CH trans out-of-flat bending), 1330 $cm^{-1}$(δ C–N stretching vibration), 1492 $cm^{-1}$ and 1594 $cm^{-1}$ (γ C–C monosubstituted phenyl) [32].

In the FTIR spectrum recorded for the BPhen layer, the characteristic vibrations at about: 742 $cm^{-1}$, 760 $cm^{-1}$ and 699 $cm^{-1}$ appear due to the C=C and C=N stretching were observed [33]. Based on these results, we can consider that no changes appear in the chemical composition of the organic materials during their deposition as thin films by MAPLE technique.

The UV-VIS spectra of the organic heterostructures prepared with LS13 and LS78 (Figure 6) are determined by the optical properties of the constituent materials (α-NPD, LS13 or LS78 and BPhen). Both organic materials (α-NPD and BPhen) are characterised by absorptions bands under 350 nm due to the π-π* electronic transition typical for the triphenylamine derivatives (α-NPD) and to the phenyl or phenanthroline moieties (BPhen), respectively [34, 35]. For the arylenevinylene oligomers, the characteristic absorption bands are located also in the UV part being attributed to the n–π* transition in the carbazole aromatic ring (LS13) or in thetriphenylamine moiety (LS78)[36, 37]. It can be noticed that P1 sample (300 nm thickness) presents a better transmittance in the visible part of the spectrum than P3 sample (400 nm thickness) and the same shape of the absorption spectrum. The UV-VIS spectra of the heterostructures prepared on flat electrode (P2 and P4) discloses similar behaviour.

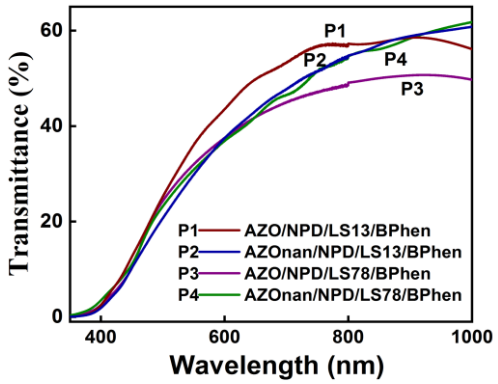


*Fig. 6. UV-VIS spectra of the prepared organic heterostructures.*

AFM investigations carried out on the organic heterostructures revealed a globular morphology having grains with different sizes for both heterostructures prepared with LS13 and LS78 (Fig. 7). In the case of the P2 and P4 samples, it can be observed that the patternation is preserved after the deposition of three organic layers. Comparing the samples prepared on flat with those obtained on patterned electrode, an increase in the Z value with ~100 nm for the samples P2 and P4 is evidenced compared to the same structure on flat electrode. The samples have been realized in the same deposition cycles. Also, an increase in the Z value is deduced for the sample P3 in comparison with the sample P1. Although, the both samples were prepared on flat electrode, the thickness of the organic intermediary layer is different, 300 nm for LS13 and 400 nm for LS78. The lowest RMS value (53 nm) is calculated for P1 prepared on flat electrode and with LS13 as intermediary layer. As was expected, the highest RMS value (95 nm) is determined for the sample P4 which is characterised by an increased thickness and is prepared on the nanostructured electrode. While the RMS value for the P4 sample is greater than that of P3, the difference in the RMS values between P4 and P3 is not so high (5 nm) compared to the difference in RMS between P2 and P1(24 nm). The higher conformational flexibility of LS78 molecules in P4 sample favours a better arrangement of these molecules in the spaces between the pillars.

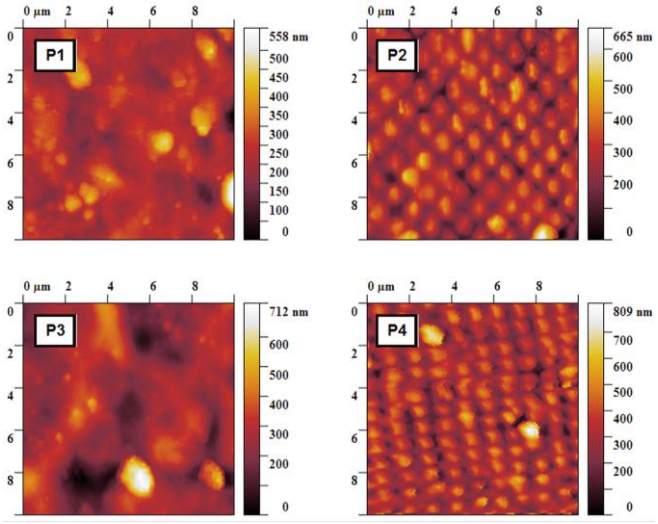


*Fig. 7. AFM 2D images of the prepared organic heterostructures.*

I-V characteristics recorded in dark of the investigated organic heterostructures (Fig. 8) are not linear. An improvement in the current value (at 1V) for the samples prepared on patterned electrode was evidenced. The best current value (~$2x10^{-5}$A) was recorded for the sample P4 based on LS78 and having AZO/NS substrate which means that such electrode is useful in the fabrication of these kinds of heterostructures. However, a diode behaviour was observed for the sample P3 prepared also with LS78 on flat electrode. Comparing the heterostructures made on the flat electrode (P1 and P3) with those made on nanostructured electrode (P2 and P4) with different intermediate organic layer (LS13 or LS78), LS78 seems to be more suitable for heterostructures with improved electrode properties. This can be explained taking into account the position of the lowest unoccupied molecular orbital (LUMO) levels in the used oligomers. Whereas the position of the highest occupied molecular orbital (HOMO) is similar for the both oligomers ($E_{HOMO}$=5.08 eV for LS78 and 5.06 for LS13 [32]), the LUMO position ($E_{LUMO}$=3.21 eV [32]) of LS78, apparently is more favourable for the charge carrier injection than that of LS13 ($E_{LUMO}$=2.95 eV [32]). The results are promising and further studies will envisage the quality of the layers contained in the heterostructures, as a factor that has a major influence on the exhibited electrical properties.

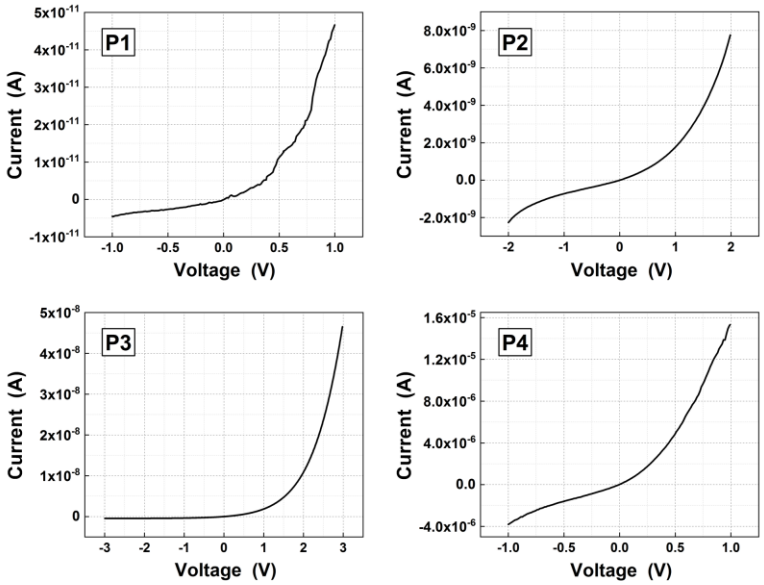


*Fig. 8. I-V characteristics of the prepared organic heterostructures.*

## 4. Conclusions

NIL process was successfully used for obtaining pillars periodic nanostructures on the glass substrate. As transparent conductive electrode, an AZO layer was deposited by PLD on these nanostructures. Further, organic heterostructures were deposited by MAPLE on AZO flat and patterned electrode. The FTIR spectra of the organic films present the vibrational bands characteristic to the raw materials. The AFM images confirm that the patternation is preserved for the samples prepared on AZO patterned electrode after the MAPLE deposition of three organic layers. An improvement in the current value was evidenced for the heterostructures fabricated on patterned electrode. We conclude that this kind of heterostructures realised with arylenevinylene oligomers LS13 and LS78 can be applied in organic device area.

**Acknowledgements**

Authors thank to A. Costas for the SEM images. The research was financially supported by the Romanian Ministry of Research and Innovation by National Core Program PN16-480103 and from ROSA STAR Contract 179/2017.

## References

[1] G. A. Torres Sevilla, M. M. Hussain, IEEE Journal on Emerging and Selected Topics in Circuits and Systems **7**, 147 (2017).
[2] R.W. Miles, G. Zoppi, I. Forbes, Mater. Today **10**, 20 (2007).
[3] C. Liu, Y. Xu, Y.-Y. Noh, Mater. Today **18**, 79 (2015).
[4] M. Socol, N. Preda, O. Rasoga, C. Breazu, I. Stavarache, F. Stanculescu, G. Socol, F. Gherendi, V. Grumezescu, N. Stefan, M.Girtan, Appl. Surf. Sci. **374**, 403 (2016).
[5] N. Yeh, P.Yeh, Renewable and Sustainable Energy Reviews **21**, 421(2013).
[6] C. Florica, A. Costas, A. Kuncser, N. Preda, I.Enculescu, Nanotechnology **27**, 475303 (2016).
[7] Y. Yang, F. Wudl, Adv. Mater. **21**, 1401(2009).
[8] F. F. Vidor, T. Meyers, U. Hilleringmann, Electronics **4**, 480 (2015).
[9] K. Jun Yu, Z.Yan, M. Han, J. A. Rogers, Flexible Electronics **1**, 1 (2017).
[10] M. Socol, N. Preda, C. Breazu, C. Florica, A. Costas, C. M. Istrate, A. Stanculescu, M. Girtan, F. Gherendi, Vacuum **154**, 366 (2018).
[11] P. Semenza, Information Display **27**, 14 (2011).
[12] C. W. Tang, S. A. Van Slyke, Appl. Phys. Lett. **51**, 913 (1987).
[13] H. Kim, A. Pique, J. S. Horwitz, H. Murata, Z. H. Kafafi, C. M. Gilmore, D. B. Chrisey, Thin Solid Films **377-378**, 798 (2009).
[14] K. Ellmer, R. Cebulla, R. Wendt, Thin Solid Films **317**, 413 (1998).
[15] W. Jia, S. Dang, H. Liu, Z. Zhang, T. Li, X.Liu, B. Xu, J.Mater. Sci. and Techn. **29**,415 (2013).
[16] F. Batool, Int. J. Adv. Res. in Comp. and Commun. Eng. **5**, 152 (2016).
[17] X. Jiang, F. L. Wong, M. K. Fung, S. T. Lee, Appl. Phys Lett. **83**, 1875 (2003).
[18] H. Hosonoa, J. Kima, Y. Todaa, T. Kamiya, S. Watanabe, PNAS Early Edition, **2016**, 201617186 (2017).
[19] A. Stanculescu, O. Rasoga, N. Preda, M. Socol F. Stanculescu, I. Ionita, A.-M. Albu, G. Socol, Ferroelectrics **389**, 159 (2009).
[20] A.P. Caricato, M. Cesaria, G. Gigli, A. Loiudice, A. Luches, M. Martino, V. Resta, A. Rizzo, A. Taurino, Appl. Phys. Lett. **100**, 073306 (2012).

[21] M. Socol, N. Preda, L. Vacareanu, M. Grigoras, G. Socol, I.N. Mihailescu, F. Stanculescu, M. Jelinek, A. Stanculescu, M. Stoicanescu, Appl. Surf. Sci. **302**, 216 (2014).
[22] Z. Chen, W. Li, R. Li, Y. Zhang, G. Xu, H. Cheng, Langmuir **29**, 13836 (2013).
[23] M. Socol, N. Preda, A. Stanculescu, C. Breazu, C. Florica, O. Rasoga, F. Stanculescu, G. Socol, Appl. Phys. A **123**, 371 (2017).
[24] F.-Z. Ghomrani, S. Iftimie, N. Gabouze, A. Serier, M. Socol, A. Stanculescu, F. Sanchez, S. Antohe, M. Girtan, Optoelectron. Adv. Mat. **5**, 247 (2011).
[25] G. Socol, M. Socol, N. Stefan, E. Axente, G. Popescu-Pelin, D. Craciun, L. Duta, C.N. Mihailescu, I.N. Mihailescu, A. Stanculescu, D. Visan, A.C. Galca, V.Craciun, Appl. Surf. Sci. **260** 42 (2012).
[26] A. S. Pugalenthi, R. Balasundaraprabhu, V. Gunasekaran, N. Muthukumarasamy, S. Prasanna, S. Jayakumar, Mater. Sci. Semicond. Process. **29,** 176 (2015).
[27] C. E. Petoukhoff, Z. Shen, M. Jain, A.M. Chang, D. M. O'Carroll, J. Photonics Energy **5**, 057002 (2015).
[28] C. Breazu, N. Preda, M. Socol, F. Stanculescu, E. Matei, I. Stavarache, G. Iordache, M. Girtan, O. Rasoga, A. Stanculescu, Dig. J. Nanomater. Biostruct. **11**, 1213 (2016).
[29] M. Socol, N. Preda, A. Stanculescu, C. Breazu, C. Florica, F. Stanculescu, S. Iftimie, M. Girtan, G. Popescu-Pelin, G. Socol, Appl. Surf. Sci. **417**, 196 (2017).
[30] J. W. Leem, J. S. Yu, Phys. Status Solidi A **208,** 2220 (2011).
[31] M. D. Halls, C.P. Tripp, H.B. Schlegel, Phys. Chem. Chem. Phys. **3**, 2131 (2001).
[32] L. Vacareanu, M. Grigoras, J. Appl. Electrochem. **40,** 1967, (2010).
[33] Y. Cao, H. Liu, Z. Yuan, G. Wei, Aust. J. Chem. **70**, 608 (2017).
[34] J. C. S. Costa, R. J. S. Taveira, C. F. R. A. C. Lima, A. Mendes, L. M. N. B. F. Santos, Opt. Mater. **58**, 51 (2016).
[35] Z. Bin, Z. Liu, P. Wei, L. Duan, Y. Qiu, Nanotechnology **27**, 174001 (2016).
[36] C.-H. Ku, C.-H. Kuo, M.-K. Leung, K.-H. Hsieh, Eur. Polym. J. **45**, 1545, (2009).
[37] V. Promarak, S. Ruchirawat, Tetrahedron **63**, 1602 (2007).